Multilayer thin-film inspection through measurements of reflection coefficients

Kai Wu,[1] Cheng-Chung Lee,[1,*] Neal J. Brock,[2] and Brad Kimbrough[2]

[1]*Department of Optics and Photonics/Thin Film Technology Center, National Central University, Chung-Li, 32001, Taiwan*

[2]*4D Technology Corporation, Tucson, Arizona 85706, USA*

**Corresponding author: cclee@dop.ncu.edu.tw*

Received June 17, 2011; revised July 10, 2011; accepted July 11, 2011;
posted July 11, 2011 (Doc. ID 149436); published August 15, 2011

A vibration-insensitive interferometer is described to measure the thickness, refraction index and surface profile of thin-film stack at normal incidence. By satisfying the continuous boundary conditions of electric and magnetic fields at interfaces in a multilayer film stack, the reflection coefficient phase of the thin-film stack can be distinguished from the phase of spatial path difference, thus thickness and refraction index can be extracted. The experiment results showed that the measurement precision is significantly increased after the phase analysis was added into the reflectance analysis. © 2011 Optical Society of America

OCIS codes: 120.3180, 120.5050, 310.6860, 310.1620.

Photometry and ellipsometry measurements are generally used to obtain the thin-film optical constants and thickness of coated elements in industries such as semiconductor, flat panel display, etc. Commercial instruments employ transmittance or reflectance spectra to learn the thin-film thickness and dispersion [1], but the precision is insufficient for multilayer thin-film measurements. Ellipsometers, which are one of the most popular instruments, offer higher precision than a spectrometer, since it not only measures reflectance but also the phase spectra. However, the measurement must be done at non-normal incidence and it is difficult to obtain two-dimensional (2D) information.

The surface profiles of the substrates are usually inspected by some other instruments, such as an atomic force microscope, a scanning electron microscope, or an optical profiler. Among these methods, optical profilers or white light interferometers can detect the surface profile without damaging the sample. If a coated element is placed in an optical interferometer test beam, the measured phase difference will be composed of two parts. The first part is the spatial path difference between reference and test beams. The second part is the reflection coefficients phase difference between the reference and test surfaces. These two parts cannot be distinguished from each other in a single wavelength measurement. A white light interferometer was used to obtain the reflection phase spectrum by utilizing a piezoelectric transducer (PZT) and fast Fourier transformation (FFT) processing [2]. The reflection phase spectrum measured by the interferometer was proven useful in determining the thin-film thickness. However, this method is vibration sensitive and not suitable for in-line examination systems. The spectral reflection phase of thin films was also extracted by appropriate positioning of a reference surface to induce a spatial carrier frequency for FFT filtering analysis [3]. But this generated an unknown offset, and the precision was limited. In other research efforts [4,5], an optical interferometer was used as a reflectance spectrometer to obtain film thickness and the phase measurement was used only for the surface profile. However, the obtained thickness precision would have been better had it utilized both the reflectance and phase spectrum. Furthermore, the precision of the surface profile obtained with FFT methods is typically lower than with phase-shifting methods since optical aberrations cannot be removed. Among these research efforts, only measurements of single-layer thin films were presented, which cannot be applied to some multilayer thin films commonly used in the industry. Furthermore, thin-film refraction indices should not be treated as known constants, since they may change even under the same process conditions. Thus, although calculated thickness precision seems higher because of much fewer unknowns, thin-film thickness was not truly obtained.

In this article, a dynamic interferometer with good immunity to vibration was used to do measurements. Both the phase and intensity reflection spectra were utilized together to calculate the refraction index and thickness of thin films for acquiring higher precision.

Figure 1 shows the measuring system layout. Narrow bandpass filters were employed to select the measuring wavelength. The polarizer can be rotated to adjust the intensity ratio between two arms and optimize the interference fringe contrast. A polarization beam splitter along with quarter-wave plates in each arm make the beams reflected from the reference plate and test sample linearly polarized and their polarization directions orthogonal to each other. After passing through the 45° quarter-wave plate in front of the imaging lens, the two beams are converted to right and left circular polarizations, respectively. These two beams then interfere

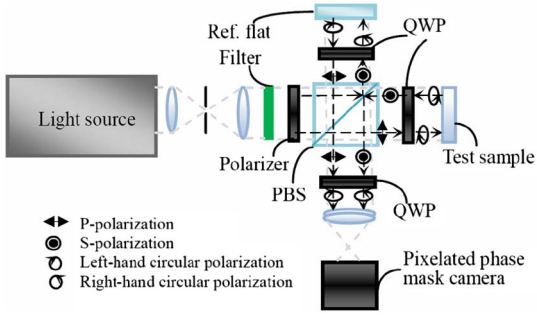

Fig. 1. (Color online) Measuring system layout. QWP, quarter-wave plate; PBS, polarization beam splitter.

with each other after passing through a linear polarizer. If the polarizer is oriented at an angle α with respect to the polarization of reference beam, the intensity can be expressed as

$$I = I_T + I_R - 2\sqrt{I_T I_R}\cos(2\alpha + \delta_m), \tag{1}$$

where I_T and I_R are the intensities coming from the test arm and reference arm, respectively. δ_m is the phase difference between the reference and test beams. The detecting element used in this system is a micropolarizer pixelated camera with adjacent pixels having different oriented polarizers on them. Four different polarizers at 0°, 45°, −45°, and 90°, respectively, on the camera, generate four different phase-shifted interferograms simultaneously. Hence, δ_m can be derived from the phase-shifting algorithm [6,7] without moving the reference arm. The vibration influence during phase acquisition, as occurs with the conventional phase shifting achieved by PZT, can thereby be avoided. The initial spatial path difference between reference and test points will be constant for all measuring wavelengths.

The phase difference we measured between the reference points would be $\delta_m = (\delta_T - \delta_R) + \delta_S$, where δ_T is the phase of the thin-film reflection coefficient, which is the summation of reflections from the interfaces inside the thin-film stack. δ_R is the reflection phase from the reference point. If the reference area is uncoated, δ_R equals π for all wavelengths. The spatial phase difference is $\delta_S = 4\pi h/\lambda$, where h is the initial spatial path difference between the reference and test points, and λ is the measuring wavelength. A portion of the test sample surface should be left uncoated as the reference area to cancel the mechanical vibration induced during narrow bandpass filters changes. However, it is not needed if the narrow bandpass filters are substituted by a dispersion element, such as a grating, prism, or acousto-optic tunable filter to enable phase measurements at different wavelengths simultaneously [3–5]. The uncoated reference substrate is generally not extremely flat and may have hundreds of nanometers greater height variation than the test substrate surface. This can be solved by utilizing multiple wavelengths because the reflection coefficient of the thin-film stack is a function of wavelength.

Consider a detecting beam normally incident to a film stack. To satisfy the electromagnetic boundary conditions at the interfaces in a single layer thin-film as shown in Fig. 2(a), we find the following equations [8]:

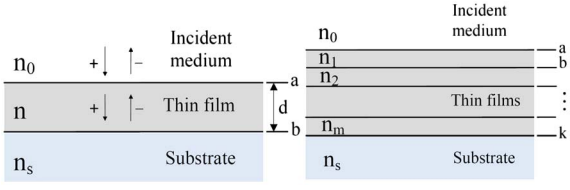

Fig. 2. (Color online) (a) Single layer thin film. (b) Multilayer thin films.

$$\begin{aligned} E_a &= E_b\cos\delta + H_b\tfrac{i}{y}\sin\delta \\ H_a &= E_b iy\sin\delta + H_b\cos\delta \end{aligned} \quad \text{or} \quad \begin{bmatrix} E_a \\ H_a \end{bmatrix} = \begin{bmatrix} \cos\delta & \frac{i}{y}\sin\delta \\ iy\sin\delta & \cos\delta \end{bmatrix}\begin{bmatrix} E_b \\ H_b \end{bmatrix}, \tag{2}$$

where E_x and H_x represent the electric and magnetic fields of incident light at interface x, respectively. y is the optical admittance of the thin film. δ is the optical phase thickness, which equals $2\pi nd/\lambda$, where d and λ are the physical thickness and measuring wavelength, respectively. The plus and minus signs indicate that the beams go downward and upward, respectively.

At interface a,

$$\begin{aligned} H_a &= H_{0a}^{+} + H_{0a}^{-} = y_0 E_{0a}^{+} - y_0 E_{0a}^{-} \\ E_a &= E_{0a}^{+} + E_{0a}^{-} \end{aligned} \quad \text{or} \quad \begin{aligned} E_{0a}^{+} &= \tfrac{y_0 E_a + H_a}{2y_0} \\ E_{0a}^{-} &= \tfrac{y_0 E_a - H_a}{2y_0} \end{aligned}, \tag{3}$$

where y_0 indicates the optical admittance in incident medium 0. For multilayer films, as shown in Fig. 2(b), Eq. (2) can be applied on every adjacent interface pair so the following equation should be satisfied [8]:

$$\begin{bmatrix} E_a \\ H_a \end{bmatrix} = M_1 M_2 \cdots M_m \begin{bmatrix} E_k \\ H_k \end{bmatrix} = \prod_{j=1}^{m} \begin{bmatrix} \cos\delta_j & \frac{i}{y_j}\sin\delta_j \\ iy_j\sin\delta_j & \cos\delta_j \end{bmatrix}\begin{bmatrix} E_k \\ H_k \end{bmatrix}. \tag{4a}$$

If we divide Eq. (4a) by E_k, the equation can be rewritten as:

$$\begin{aligned} \begin{bmatrix} B \\ C \end{bmatrix} &= \begin{bmatrix} \frac{E_a}{E_k} \\ \frac{H_a}{E_k} \end{bmatrix} = \prod_{j=1}^{m} \begin{bmatrix} \cos\delta_j & \frac{i}{y_j}\sin\delta_j \\ iy_j\sin\delta_j & \cos\delta_j \end{bmatrix}\begin{bmatrix} 1 \\ \frac{H_k}{E_k} \end{bmatrix} \\ &= \prod_{j=1}^{m} \begin{bmatrix} \cos\delta_j & \frac{i}{y_j}\sin\delta_j \\ iy_j\sin\delta_j & \cos\delta_j \end{bmatrix}\begin{bmatrix} 1 \\ y_s \end{bmatrix} \\ &= \prod_{j=1}^{m} \begin{bmatrix} \cos\delta_j & \frac{i}{n_j y_v}\sin\delta_j \\ in_j y_v\sin\delta_j & \cos\delta_j \end{bmatrix}\begin{bmatrix} 1 \\ n_s y_v \end{bmatrix}, \end{aligned} \tag{4b}$$

where we set $E_a/E_k = B$ and $H_a/E_k = C$. δ_j and y_j represent the phase thickness and optical admittance in the jth medium, respectively. n_j is the refraction index of medium j. y_v is the optical admittance in vacuum. The reflection coefficient of thin film is

$$re^{i\delta_T} = \frac{E_{0a}^{-}}{E_{0a}^{+}} = \frac{y_0 E_a - H_a}{y_0 E_a + H_a} = \frac{n_0 y_v B - C}{n_0 y_v B + C}, \tag{5}$$

where all y_v terms will be canceled in the final calculations of Eq. (4). From Eqs. (4b) and (5), we can know that both r and δ_T are functions of n_j, d_j, and λ. Because the light is at normal incidence, the reflection coefficient mathematic expression is much simpler than that in the oblique incidence case. For a thin film with absorption, n_j in Eq. (2) should be replaced by $n_j - ik_j$ [8], where k_j is the extinction coefficient of the jth layer film. The term r is equal to the square root of thin-film reflectance R. If the reference arm is blocked, the reflectance R can

be measured by comparing the detected reflection intensity of the test specimen and a reference specimen of which reflectance at each wavelength is already obtained before the test. Then, by minimizing the following error function, the $n_{j(\lambda)}$, d_j, and h can be found:

$$E(\delta_T, \delta_S, r) = \sum_{i=1}^{w} \{|\delta_m(\lambda_i) - [\delta_T(n_{1(\lambda_i)} \ldots n_{m(\lambda_i)}, d_1 \ldots d_m, \lambda_i) - \delta_R(\lambda_i) + \delta_S(h, \lambda_i)]|^2 + |\eta[r_m(\lambda_i) - r(n_{1(\lambda_i)} \ldots n_{m(\lambda_i)}, d_1 \ldots d_m, \lambda_i)]|^2\}, \quad (6)$$

where δ_m and r_m are the measured reflection magnitude and measured total phase, respectively. δ_T and r can be derived from models described in Eqs. (3)–(5). Cauchy's Equation was applied for fitting the dispersion of the refraction indices. The genetic algorithm was employed to find the answers to Eq. (6). Since reflection phase and magnitude are in different units and dimensions, η is a weighting factor, which should be adjusted to let them have about the same value. Its value is not limited or critical. As the wavelength is changed, the spatial path difference phase δ_S will be simply changed by a wavelength factor, that is, $\delta_S' = (\lambda/\lambda')\delta_S$, where λ and λ' are the original and current measuring wavelengths, respectively. On the other hand, δ_T is a nonlinear function of wavelength, as described in Eqs. (4) and (5). Thus, δ_S and δ_T can be distinguished from each other by multiwavelength measurements.

A 200 W mercury lamp light source was used in the interferometer, and the whole system was set on a table without any antivibration mechanism. The test sample was a transparent BK7 glass substrate of 1 mm thickness with two waves flatness and coated with two thin-film layers of SiO_2 (first layer) and Ta_2O_5 (second layer). The films were prepared by ion beam sputtering deposition. Narrow bandpass filters with 10 nm spectrum bandwidth were used to select measuring wavelengths. Only eight wavelengths, 532, 550, 580, 589, 630, 656, 690, and 710 nm, were used for measurements. The experimental results are compared with ellipsometer measurements and shown in Table 1. A Sopra GES5 ellipsometer was employed to perform measurements every 5 nm from 450 to 800 nm.

The averages and standard deviations (SDs) of thickness d and the refraction index at 630 nm $n_{(630)}$ measurement results are listed in Table 1 for comparison. The statistics come from 50 measurements under the same conditions. One can see that using only reflectance data results in a large standard deviation (low precision) and low accuracy. This is because the measurement data are obviously too few and insufficient for numerical fitting. However, after the optical phase measurement data were included in the calculations, the precision significantly improved and the results are similar to the ellipsometer results. The optical phase values measured by the interferometer indeed help us to obtain more precise results. Notice that the precision will be further improved when more wavelengths are used for measurement.

Table 1. Experimental Results Comparisons

		Ellipsometer	Reflectance Only (Avg./SD)	Reflectance and Phase (Avg./SD)
First layer	d	93 nm	80 nm/6.89%	90 nm/1.45%
	$n_{(630)}$	1.48	1.65/4.13%	1.48/0.79%
Second layer	d	98 nm	95 nm/3.52%	98 nm/0.89%
	$n_{(630)}$	2.14	1.89/3.91%	2.15/1.20%

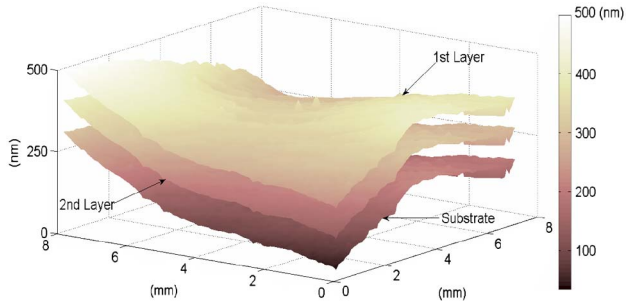

Fig. 3. (Color online) Result of volumetric profile of thin-film stack measurement.

Since this system can do measurements under normal incidence and the detecting element is a 2D CCD array, the whole profile of the element can be measured at the same time. Figure 3 shows the profile obtained with our measurement apparatus located on a table without antivibration mechanism. It shows that the coated film has high compress stress, which is consistent with the result measured by other interferometers [9].

With appropriate magnification optics, the measurement area can be enlarged to provide high-precision measurement of any curved or patterned thin-film coated substrate.

In conclusion, a simple, vibration-insensitive interferometer was developed to measure the properties of thin-film elements. The refractive index and thickness of thin films were determined by measuring the reflection phase in addition to the reflection magnitude, which resulted in significantly higher precision. The system combines two capabilities, surface profiling and thin-film inspection, which can be further developed as an in-line inspection system for various applications, such as thin-film photovoltaic, semiconductor, flat panel display, biomedical specimen, and so on.

The authors thank J. C. Wyant for his valuable advice and the National Science Council of Taiwan (NSCT) for providing financial support under project NSC 099-2221-E-008-046-MY3.

References

1. K. P. Vitaly, F. V. Valery, and H. Vitali, Appl. Opt. **45**, 4547 (2006).
2. S. W. Kim and G. H. Kim, Appl. Opt. **38**, 5968 (1999).
3. D. S. Kim, S. H. Kim, H. J. Kong, and Y. W. Lee, Opt. Lett. **27**, 1893 (2002).
4. Y. S. Ghim and S. W. Kim, Appl. Phys. Lett. **91**, 091903 (2007).
5. Y. S. Ghim and S. W. Kim, Appl. Opt. **48**, 799 (2009).
6. N. Brock, J. Hayes, B. Kimbrough, J. Millerd, M. North-Morris, M. Novak, and J. C. Wyant, Proc. SPIE **5875**, 58750F (2005).
7. J. Millerd, N. Brock, J. Hayes, B. Kimbrough, M. Novak, M. North-Morris, and J. C. Wyant, Proc. SPIE **5856**, 14 (2005).
8. H. A. Macleod, *Thin Film Optical Filters*, 3rd ed. (Institute of Physics Publishing, 2001).
9. C. C. Lee, C. L. Tien, W. S. Sheu, and C. C. Jaing, Rev. Sci. Instrum. **72**, 2128 (2001).